Human Reproduction, Vol.35, No.5, pp. 1145–1158, 2020
Advance Access Publication on May 6, 2020 doi:10.1093/humrep/deaa077

human reproduction

ORIGINAL ARTICLE ***Reproductive endocrinology***

Metformin inhibits testosterone-induced endoplasmic reticulum stress in ovarian granulosa cells via inactivation of p38 MAPK

Jiamin Jin[1,2,†], Yerong Ma[1,2,†], Xiaomei Tong[1,2], Weijie Yang[1,2], Yongdong Dai[1,2], Yibin Pan[1,2], Peipei Ren[1,2], Liu Liu[1,2], Heng-Yu Fan[2,3], Yinli Zhang[1,2,*], and Songying Zhang[1,2,*]

[1]Assisted Reproduction Unit, Department of Obstetrics and Gynecology, Sir Run Run Shaw Hospital, Zhejiang University School of Medicine, 310016, Hangzhou, China., [2]Department of Obstetrics and Gynecology, Key Laboratory of Reproductive Dysfunction Management of Zhejiang Province, 310016, Hangzhou, China., [3]Life Sciences Institute, Zhejiang University, 310058, Hangzhou, China.

*Correspondence address. Songying Zhang, Assisted Reproduction Unit, Department of Obstetrics and Gynecology, Sir Run Run Shaw Hospital, No. 3 Qingchun East Road, Jianggan District, Hangzhou 310016, China. Tel: +86 13805727588; Fax: +86 0571 86044817; E-mail: zhangsongying@zju.edu.cn and Yinli Zhang, Assisted Reproduction Unit, Department of Obstetrics and Gynecology, Sir Run Run Shaw Hospital, No. 3 Qingchun East Road, Jianggan District, Hangzhou 310016, China. Tel: +86 15267073236; E-mail: zhangyinli@zju.edu.cn

Submitted on June 3, 2019; resubmitted on March 10, 2020; accepted on March 25, 2020

STUDY QUESTION: Does metformin inhibit excessive androgen-induced endoplasmic reticulum (ER) stress in mouse granulosa cells (GCs) *in vivo* and *in vitro*?

SUMMARY ANSWER: Metformin inhibits testosterone-induced ER stress and unfolded protein response (UPR) activation by suppressing p38 MAPK phosphorylation in ovarian GCs.

WHAT IS KNOWN ALREADY: Polycystic ovary syndrome (PCOS) is associated with hyperandrogenism. Excessive testosterone induces ER stress and UPR activation in human cumulus cells, leading to cell apoptosis. Metformin has potential inhibitory effects on ER stress and UPR activation, as demonstrated in human pancreatic beta cells and obese mice.

STUDY DESIGN, SIZE, DURATION: Cumulus cells and follicular fluid were collected from 25 women with PCOS and 25 controls at our IVF centre. A dihydrotestosterone (DHT)-induced PCOS mouse model was constructed and treated with or without metformin. Primary mouse GCs and cumulus-oocyte complexes (COCs) were cultured with testosterone, metformin, a p38 MAPK inhibitor, or p38 MAPK small interfering RNA.

PARTICIPANTS/MATERIALS, SETTING, METHODS: The levels of UPR sensor proteins and UPR-related genes were measured in cumulus cells from PCOS and control patients by real-time quantitative PCR (qPCR) and western blot. The ovaries, oocytes, GCs and COCs were collected from PCOS mice treated with metformin and controls. The expressions of ER stress markers and p38 MAPK phosphorylation were assessed by qPCR, western blot and immunofluorescence. A subsequent *in vitro* analysis with primary cultured GCs and COCs was used to confirm the influence of metformin on ER stress activation by qPCR and western blot. Finally, the effects of ER stress activation on GCs and COCs in relation to LH responsiveness were examined by qPCR and COC expansion.

MAIN RESULTS AND THE ROLE OF CHANCE: The expression of the ER stress markers *GRP78*, *CHOP* and *XBP1s* in the cumulus cells was higher in PCOS patients than in control patients, as were the levels of the UPR sensor proteins p-IRE1α, p-EIF2α and GRP78. Compared to those of control mice, the ovaries, GCs and COCs of DHT-treated PCOS mice showed increased levels of ER stress marker genes and proteins. Hyperandrogenism in PCOS mouse ovaries also induced p38 MAPK phosphorylation in COCs and GCs. Metformin inhibited ER stress activation was associated with decreased p-p38 MAPK levels. *In vitro* experiments, testosterone-induced ER stress was mitigated by metformin or p38 MAPK inhibition in primary cultured GCs and COCs. COCs expanded rapidly in the presence of testosterone during LH administration, and ovulation-related genes, namely, *Areg*, *Ereg*, *Ptgs2*, *Sult1e1*, *Ptx3* and *Tnfaip6*, were strongly expressed in the COCs and GCs. These effects were reversed by treatment with metformin, an ER stress inhibitor or by knockdown of p38 MAPK.

LIMITATIONS, REASONS FOR CAUTION: The number of PCOS patients in this study was small.

†The authors consider that the first two authors should be regarded as joint first authors.

WIDER IMPLICATIONS OF THE FINDINGS: This study provides further evidence for metformin as a PCOS treatment.

STUDY FUNDING/COMPETING INTEREST(S): This study was funded by the National Key Research and Developmental Program of China (2018YFC1004800), the Key Research and Development Program of Zhejiang Province (2017C03022), the Zhejiang Province Medical Science and Technology Plan Project (2017KY085, 2018KY457), the National Natural Science Foundation of China (31701260, 81401264, 81701514), and the Special Funds for Clinical Medical Research of the Chinese Medical Association (16020320648). The authors report no conflict of interest in this work and have nothing to disclose.

TRIAL REGISTRATION NUMBER: N/A.

Key words: PCOS / testosterone / ER stress / metformin / p38 MAPK

Introduction

Polycystic ovary syndrome (PCOS) is very common in women of reproductive age, affecting 4–21% of these women worldwide, depending on the diagnostic criteria applied. According to statistical data from 2008 to 2014, the prevalence of PCOS is lower in China, at ~2–11% (Bozdag *et al*. 2016; Lizneva *et al*. 2016). PCOS is a heterogeneous disease, involving metabolic and endocrine disorders and is characterized by various symptoms, including hyperandrogenism, insulin resistance, ovulation dysfunction and gonadotropin disorder. Although the underlying pathogenesis of PCOS is unclear, this disease is thought to be associated with oxidative stress, chronic low-grade inflammation, mitochondrial dysfunction and metabolic disorders, which impair normal ovarian function (Qiao and Feng, 2011; Insenser *et al*., 2013; Barrea *et al*., 2018; Jia *et al*., 2019).

Metformin was originally used to treat both obese and non-obese women with PCOS because of its ability to decrease hyperandrogenism. This effect of metformin on steroid production was initially thought to result from its ability to enhance insulin sensitivity and reduce hyperinsulinaemia (Nestler and Jakubowicz, 1996). Subsequent studies showed that inhibition of electron transport in mitochondrial respiratory complex I might be another way by which metformin lowered ovarian steroidogenesis (El-Mir *et al*., 2000; Hirsch *et al*., 2012; Kurzthaler *et al*., 2014). The latter mechanism has also been implicated in other organs and tissues (El-Mir *et al*., 2000; Miller *et al*., 2013). More recent studies have shown that despite the ability of metformin to reduce androgen levels in PCOS patients, its effects regarding restoration of fertility, improved live birth rate and menstrual irregularity are not consistent among PCOS patients (Naderpoor *et al*., 2016; Sam and Ehrmann, 2017; Luque-Ramirez *et al*., 2018). Thus, further studies are needed to obtain additional insight into the mechanisms of action of metformin to make the treatment successful in all PCOS patients.

Most proteins are synthesized and processed in the endoplasmic reticulum (ER) before becoming functional. In the ER, proteins are folded into specific three-dimensional structures with unique posttranslational modifications. However, when the protein-folding capacity of the ER is negatively affected, a situation named ER stress may occur (Walter and Ron, 2011). To reduce ER stress, signal transduction pathways called the unfolded protein response (UPR) are activated (Kozutsumi *et al*., 1988; Shore *et al*., 2011). UPR is mediated by three canonical sensor proteins: inositol-requiring enzyme 1 (IRE1), protein kinase-like ER kinase (PERK) and activating transcription factor 6 (ATF6). They are transmembrane proteins and bind with the ER chaperone 78-kDa glucose-regulated protein (GRP78), under non-stressed conditions. When ER stress occurs, they are separated from GRP78 and activated. Activated IRE1α removes a small intron of unspliced X box-binding protein 1 (*XBP1u*) resulting in spliced XBP1 (*XBP1s*). Meanwhile, PERK phosphorylates eukaryotic translation initiation factor 2α (eIF2α) to attenuate ER protein overload by inducing transcription of *ATF4*. The ATF6 activation induces transcription of C/EBP homologous protein (*CHOP*) and *GRP78*. The increased GRP78/*GRP78*, p-eIF2α, p-IRE1α, *XBP1s*, *ATF4* and *CHOP* are commonly used as markers of ER stress or UPR activation (Maurel *et al*., 2014; Wang and Kaufman, 2016).

ER stress and UPR activation play important roles in the development and pathogenesis of human diseases, especially genetic disorders, metabolic dysfunction, autoimmune diseases, neurodegenerative diseases and cancer (Oakes and Papa, 2015; Wang and Kaufman, 2016). Recent studies have shown that ER stress occurs in ovarian cells, affecting oocyte maturation, follicle formation and ovulation (Cree *et al*., 2015; Lee *et al*., 2017; Wu *et al*., 2017; Park *et al*., 2018; Vasickova *et al*., 2018; Liu *et al*., 2019). Few studies have reported the relationships between ER stress and human ovarian diseases. Excessive androgens activate ER stress in granulosa cells (GCs), eventually promoting apoptosis via death receptor 5 (Azhary *et al*., 2019). However, the mechanism by which androgens activate ER stress and whether metformin by decreasing ER stress has a beneficial effect in PCOS patients is still unclear.

Thus, we sought to determine whether metformin alleviates hyperandrogenism-induced ER stress in PCOS. First, we determined whether ER stress levels were higher in cumulus cells derived from PCOS patients and dihydrotestosterone (DHT)-induced PCOS mice than in corresponding controls. We found that ER stress was activated in cumulus cells from PCOS patients. We also found that ER stress was activated in GCs, cumulus–oocyte complexes (COCs) and cumulus cells but not in oocytes from PCOS mice. Then, we evaluated the inhibitory effects of metformin on ER stress and characterized the underlying mechanisms of actions of metformin in GCs and COCs by *in vivo* and *in vitro* studies. Furthermore, we examined the effects of testosterone, metformin and p38 MAPK on COC expansion and relative gene expression in primary cultured cells.

Materials and Methods

Human specimens

Control subjects (n = 25) and patients with PCOS (n = 25) were recruited from *in vitro* fertilization (IVF) laboratories at the Sir Run Run Shaw Hospital, Hangzhou, Zhejiang, China. All recruited patients signed informed consent forms, and all experimental procedures were approved by our hospital Ethics Committee. The PCOS patients were

recruited based on the Rotterdam PCOS Diagnostic Criteria (showing two of the following signs: oligo- or anovulation, clinical and/or biochemical hyperandrogenism, and polycystic ovaries on ultrasound) after exclusion of related disorders (Rotterdam, 2004). The control group consisted of patients seeking IVF assistance for male infertility ($n = 25$). The control patients were confirmed by ultrasound to have normal ovarian morphology and normal ovulatory cycles with endocrine indicators. Additionally, patients who had taken metformin before or during IVF treatments were excluded. The levels of anti-Müllerian hormone (AMH), LH, FSH, oestradiol (E2), progesterone (P4) and total testosterone (TT) between Days 3 and 5 of the menstrual cycle were measured in all subjects. Age, infertility duration, menstrual cycle length, BMI, triglycerides (TGC), total cholesterol (CHOL), fasting glucose (FG), fasting insulin (FI) and homeostasis model assessment of insulin resistance (HOMA-IR) data were also recorded.

Cumulus cells and follicular fluid were aspirated from the subjects during oocyte retrieval. The cumulus cells were washed twice with phosphate-buffered saline (PBS) and lysed for RNA and protein extraction. Follicular fluid was collected for analysis of TT levels with a UniCel DxI 800 Access Immunoassay System (Beckman Coulter, Brea, CA, USA) in a clinical laboratory.

DHT-treated mouse model

Female wild-type C57BL/6J mice were obtained from the Animal Center of Sir Run Run Shaw Hospital. The animals were housed under standard conditions, and the experiments were performed with the permission of the hospital Ethics Committee.

On postnatal day 21, mice with similar body weights were randomly divided into DHT-treated and control groups ($n = 8$ per group). In the PCOS model group, the mice were implanted subcutaneously with DHT-releasing implants. These implants were produced by loading 1-cm silastic implants (internal diameter 1.47 mm, external diameter 1.95 mm, 508–006; Dow Corning, Midland, MI, USA) with ~10 mg of DHT (Selleck, Shanghai, China) in accordance with the methods in previous studies (Caldwell *et al*., 2017). Blank implants were implanted into the subcutaneous tissues of the mice in the control group. In another experiment, mice were divided into four groups ($n = 20$, per group). Two groups were implanted with blank or DHT implants drinking water daily. The other two groups were embedded with blank or DHT implants and were given daily water containing metformin at a concentration designed to deliver a dose of 500 mg/kg body weight/day; MedChemExpress Company, Monmouth Junction, NJ, USA).

Vaginal smears were examined daily for 2 weeks beginning at 13 weeks of age. Insulin tolerance tests (ITTs) and oral glucose tolerance tests (oGTTs) were performed at the age of 15 weeks, in line with the methods in previous studies (Caldwell *et al*., 2017). At 16 weeks of age, the mice were euthanized by carbon dioxide overdose, as indicated by the Animal Care Society of China (http://animal.sibcb.ac.cn/default.aspx?xmls=web/index.html). The body weights of the mice were recorded, and blood samples were collected. Ovaries, parametrial fat-pads, denuded oocytes and GCs were also collected, with no stimulation of ovulation. Fully grown, non-expanded COCs were harvest from mice after injection with pregnant mare serum gonadotrophin (PMSG; 5 IU per 10 g of body weight) for 44 h. The model mice were injected with human chorionic gonadotropin (hCG; 5 IU per 10 g of body weight) for 16 h to induce production of metaphase II (MII) oocytes, which were acquired at the age of 16 weeks. The PMSG and hCG were purchased from Ningbo Sansheng Pharmaceutical Co. (Ningbo, China).

Primary cell cultures and treatments

Primary cell cultures

To harvest COCs and GCs, immature mice (21 days old) were killed 44 h after intraperitoneal injection of 5 IU of PMSG, as described previously (Zhang *et al*., 2013). Antral follicles were punctured with a 26.5-G needle to release COCs and GCs. The COCs were then cultured in IVM medium (EasyCheck Company, Nanjing, China). The GCs were cultured with DMEM/F12 (Invitrogen, Carlsbad, CA, USA) supplemented with 5% (v/v) foetal bovine serum (FBS; Gibco, Waltham, MA, USA) and 1% (v/v) penicillin and streptomycin (Meilunbio, Dalian, Shandong, China).

GC treatments

To evaluate the role of metformin on hyperandrogenism-induced ER stress, the GCs were pre-treated with 10 μM testosterone (MedChemExpress Company, Monmouth Junction, NJ, USA) and 1 mM metformin for 24 h. The concentration of metformin was based on previous studies (Lee *et al*., 2005; Samuel *et al*., 2017). For determining the role of p38 MAPK in hyperandrogenism-induced ER stress, the GCs were pre-treated with the p38 MAPK inhibitor SB203580 (10 μM; Cell Signaling Technology, Boston, MA, USA) for 2 h and then incubated with 10 μM testosterone for another 24 h. Forskolin (FSK, 10 μM; Med Chem Express Company, Monmouth Junction, NJ, USA) and phorbol 12-myristate 13-acetate (PMA, 20 nM; Med Chem Express Company, Monmouth Junction, NJ, USA) were used to mimic LH stimulation (Zhang *et al*., 2014). To determine the effect of ER stress activation on LH responsiveness, the GCs were treated with FSK/PMA for 4 h after treatments of 10 μM testosterone, 1 mM metformin and ER stress inhibitor tauroursodeoxycholic acid (TUDCA, 1 mg/ml; Med Chem Express Company, Monmouth Junction, NJ, USA) for 24 h. Meanwhile, the GCs also treated with ER stress inducer thapsigargin (TG, 1 μM; Cell Signaling Technology, Boston, MA, USA) for 1 h before its treatment with FSK/PMA for 4 h.

COC treatments

The COCs were cultured in IVM medium with 10 μM testosterone, 1 mM metformin, 10 μM SB203580, 1 mg/ml TUDCA for 16 h or with 1 μM TG for 1 h. COC expansion areas were measured by ImageJ software (National Institutes of Health, USA) after indicated treatments.

Western blot analysis

Proteins were extracted from tissues and cells and resolved by SDS-PAGE. After the proteins had been transferred to polyvinylidene difluoride (PVDF) membranes (Millipore Corp., Billerica, MA, USA), the membranes were incubated with primary antibodies overnight at 4°C. The membranes were then incubated with horseradish peroxidase-linked anti-rabbit or anti-mouse IgG secondary antibodies (7074 or 7076, dilution: 1:2000; Cell Signaling Technology, Boston, MA, USA) and visualized by enhanced chemiluminescence (WBKLS0500; Millipore Corp., Billerica, MA, USA).

Antibodies against 78-kDa glucose-regulated protein (GRP78; ab21685, dilution: 1:1000) and phospho-inositol requiring enzyme 1α (p-IRE1α; ab48187, dilution: 1:1000) were purchased from Abcam (Cambridge, UK). Antibodies against phospho-p38 mitogen-activated protein kinase (p-p38 MAPK (Thr180/Tyr182); 9215, dilution: 1:1000), total p38 MAPK (9212, dilution: 1:1000), poly ADP-ribose polymerase (PARP; 9532, dilution: 1:1000) and phospho-eukaryotic initiation factor 2α (p-EIF2α; 3398, dilution: 1:1000) were purchased from Cell Signaling Technology (Boston, MA, USA). Antibodies against β-actin (60 008, dilution: 1:2000) and total EIF2α (11 233, dilution: 1:1000) were purchased from the Proteintech Group (Chicago, IL, USA).

ImageJ software was used to quantify the intensities of the western blot bands.

RNA isolation and real-time quantitative PCR

Total RNA was isolated from the cumulus cells of the patients with a RNeasy Plus Micro Kit (74034; Qiagen, Hilden, Germany) in accordance with the manufacturer's protocol. Total RNA was extracted from primary cultured mouse ovarian GCs and COCs and from mouse ovary-derived GCs and COCs with TRIzol Reagent (Invitrogen, Carlsbad, CA, USA). The total RNA (1 μg) was reverse-transcribed with HiScript II Reverse Transcriptase (R201-1; Vazyme, Nanjing, China). Real-time quantitative PCR (qPCR) was performed with Bestar Sybr-Green qPCR Mastermix (DBI Bioscience, Germany) on an Applied Biosystems 7500 Real-time qPCR System (Applied Biosystems, Foster City, CA, USA). The relative gene expression levels were compared with those in the controls, and all real-time qPCRs were performed in triplicate. The primers are shown in Supplementary Table SI.

Histology and immunofluorescence

Model mice were super-ovulated, MII oocytes were collected from some and fixed in 3.8% (w/v) paraformaldehyde, ovaries were collected from others, fixed in 4% (w/v) paraformaldehyde and embedded in paraffin using routine procedures. The ovaries were then sectioned at 5 μm and stained with haematoxylin and eosin. The ovarian sections were dewaxed and treated with 0.01% (w/v) sodium citrate for 20 min for antigen retrieval. The MII oocytes and sections were permeabilized with PBS containing 0.5% Triton X-100 (PBST; v/v) for 20 min and incubated for 1 h with blocking buffer (PBST containing 1% (w/v) or 5% (w/v) bovine serum albumin for MII oocytes or sections, respectively). The MII oocytes were then probed with a fluorescein-isothiocyanate (FITC)-conjugated anti-α-tubulin antibody (F2168, dilution: 1:50; Sigma Aldrich, St. Louis, MO, USA) and an anti-GRP78 antibody (dilution: 1:200) overnight at 4°C. The sections were sequentially probed with GRP78 and cleaved-caspase 3 (9661, dilution: 1:400; Cell Signaling Technology, Boston, MA, USA) primary antibodies overnight at 4°C, and then with an Alexa Fluor 594-conjugated and 488-conjugated secondary antibody (dilution: 1:200; Yeasen, Shanghai, China) for 1 h. The slides were then counterstained with 4′,6-diamidino-2-phenylindole (DAPI; 1 μg/ml; Roche, Switzerland). Digital images were acquired with a fluorescence confocal microscope (TCS SP8; Leica, Germany).

ImageJ software was used to quantify the fluorescence intensities of the immunofluorescence (IF) images.

Small interfering RNA transfection

To knock down p38 MAPK expression, GCs and COCs cultured in 24-well plates were transfected with small interfering RNAs (siRNAs) targeting p38 MAPK (si-p38) or negative control siRNA (si-nc) by means of Lipofectamine™ 3000 Transfection Reagent (L3000015; Thermo Fisher Scientific, Waltham, MA, USA) in accordance with the manufacturer's instructions. These siRNAs were purchased from RiboBio Co., Ltd (Guangzhou, China). The si-p38-1 and si-p38-2 sequences were 5′-CGTTCTACCGGCAGGAGCT-3′ and 5′-CATAATTCACAGGGACCTA-3′, respectively, and the negative control sequence for si-p38 was 5′-UUCUCCGAACGUGUCACGU-3′.

Flow cytometry

The apoptosis rates of primary cultured GCs treated with or without 10 μM testosterone were assessed by flow cytometry with Alexa Fluor 488-conjugated annexin V and propidium iodide (PI) (V13245; Thermo Fisher Scientific, Waltham, MA, USA). The experiments were performed in accordance with the manufacturer's instructions. FITC-Annexin V-positive cells were considered apoptotic cells.

Terminal deoxynucleotidyl transferase-mediated dUTP nick-end labelling assays

Transferase-mediated dUTP nick-end labelling (TUNEL) assays were performed to detect DNA fragmentation in ovary sections from DHT-treated mice and control mice. An Alexa Fluor 488 TUNEL Apoptosis Detection Kit (40307ES20; Yeasen, Shanghai, China) was used based on the provided protocol. Slides treated with DNase I for 30 min served as positive controls. DAPI was used to stain the nuclei.

Statistical analyses

IBM SPSS 23.0 (SPSS Inc., Chicago, IL, USA) was used for all statistical analyses. The demographic and clinic characteristics data for the patients are reported as means ± SEMs, except that the HOMA-IR data are presented as medians (25th–75th percentile). All continuous parameters and quantitative data are shown as means ± SEMs for different groups and were evaluated by unpaired *t* tests after normality assessment by the Kolmogorov–Smirnov test. Two-way ANOVA followed by Fisher's least significant difference multiple-comparison post hoc tests was performed to determine the significance of the differences in the area under the curve (AUC) values from the oGTTs and ITTs. $P < 0.05$ was considered to indicate significance.

Results

ER stress is strongly activated in cumulus cells from PCOS patients

To determine whether ER stress is induced by hyperandrogenism, cumulus cell and follicular fluid were collected from PCOS and normal ovulatory patients undergoing IVF/intracytoplasmic sperm injection (ICSI). There were no notable differences between the groups in terms of age, BMI, infertility duration, or serum FSH, E2, P4 and TT levels on Days 3–5 of the menstrual cycle (Table I). However, the menstrual cycle length was significantly longer in the PCOS patient

Table I Demographic data and clinic characteristics of participants.

Parameters	Control ($n = 25$)	PCOS ($n = 25$)	P value[b]
Age (years)	29.28 ± 4.43	28.88 ± 3.24	0.122
BMI (kg/m^2)	21.06 ± 2.57	22.13 ± 2.50	0.112
Infertility duration (years)	2.68 ± 2.16	3.06 ± 1.92	0.382
Cycle length (days)	31.76 ± 3.43	52.16 ± 29.68	0.001
Anti-Müllerian hormone (ng/ml)	4.83 ± 2.02	11.95 ± 6.27	0.000
Baseline LH (IU/l)	3.72 ± 1.84	10.20 ± 6.80	0.007
Baseline FSH (IU/l)	6.81 ± 1.94	6.44 ± 1.64	0.383
LH/FSH	0.54 ± 0.22	1.60 ± 1.04	0.004
Baseline total testosterone (ng/ml)	0.48 ± 0.13	0.70 ± 0.29	0.054
Baseline oestradiol (ng/l)	79.86 ± 99.52	50.32 ± 32.90	0.121
Baseline progesterone (pg/l)	14.27 ± 5.29	17.77 ± 18.01	0.181
Triglycerides (mmol/l)	0.8 ± 0.5	1.2 ± 0.6	0.011
Total cholesterol (mmol/l)	4.5 ± 1.1	5.2 ± 1.2	0.021
Fasting glucose (mmol/l)	4.9 ± 0.4	5.9 ± 1.1	0.025
Fasting insulin (μU/ml)	4.9 ± 1.0	7.2 ± 1.1	0.010
HOMA-IR[a] median (quartiles)	1.0 (0.7, 1.4)	1.9 (1.4, 2.6)	0.026
Total testosterone in follicular fluid (ng/ml)	7.95 ± 2.48	11.34 ± 4.47	0.001

Data are mean ± SEM unless stated otherwise
[a]HOMA-IR, homeostasis model assessment of insulin resistance.
[b]Unpaired t test

group than in the control group. The serum LH and AMH levels and LH/FSH ratios were significantly higher in the PCOS patients than in the control subjects. Overall, 60% of PCOS patients and 12% of control patients had TT levels higher than 0.70 ng/ml, which is the upper threshold of normal TT in our hospital. However, the average serum TT levels of PCOS and control patients were not significantly different (0.48 ± 0.13 ng/ml versus 0.70 ± 0.2 ng/ml, $P = 0.054$). Furthermore, the follicular fluid TT levels of PCOS patients were significantly higher than those of control patients (Table I). In addition, the TGC, CHOL, FG, FI and HOMA-IR levels were higher in the PCOS groups than in the control groups (Table I).

The expression of *GRP78*, *XBP1s* and *CHOP* was elevated in the cumulus cells of the PCOS patients (Fig. 1A). As shown by western blot results, the protein levels p-IRE1α, p-EIF2α and GRP78 were higher in the cumulus cells from the PCOS patients than in those from the control subjects (Fig. 1B and C).

ER stress is activated in GCs and COCs but not in oocytes in DHT-treated PCOS mice

A PCOS mouse model was established to examine the relationship between ER stress and testosterone in ovaries. A schematic of the animal model experiments is shown in Supplementary Fig. S1A. The body weights and serum steroid levels of the mice are shown in Supplementary Table SII. The PCOS group exhibited reduced P4 levels, increased DHT levels and increased body weights. The PCOS mice also lacked oestrous cyclicity and had larger cystic follicles and fewer corpora lutea (CLs) than the control mice (Supplementary Fig. S1B–E). Analysis of metabolic parameters showed that the mice with DHT-induced PCOS had larger adipocyte areas than the control mice (Supplementary Fig. S2A and B). However, there were no significant differences in oGTT or ITT results between these groups (Supplementary Fig. S2C–F). Higher CHOL and TGC levels were observed in the DHT group than in the control group (Supplementary Fig. S2G and H).

Ovaries, COCs, denuded oocytes and GCs were collected from control and PCOS mice. The expression of ER stress marker genes and UPR sensor proteins was measured. *GRP78*, *CHOP* and *XBP1s* mRNA levels were significantly increased in PCOS mouse ovaries. The transcript levels of *GRP78* and *XBP1s* were also increased in the COCs of PCOS mice, whereas the mRNA levels of *GRP78*, *CHOP*, *XBP1s* and *ATF4* were increased in the GCs of these mice (Fig. 2A). However, the levels of these mRNAs and sensor proteins in oocytes did not differ markedly between the two groups (Fig. 2A and B). Meanwhile, the mRNA levels of *XBP1u* were not changed in all samples. To confirm that ER stress was activated in the PCOS mouse ovaries, immunofluorescence was used to analyse the distribution and intensity of GRP78. The signals for GRP78 were stronger in GCs from PCOS mouse ovaries than in those from control mouse ovaries (Fig. 2C–E). Western blot analysis showed that the levels of ER stress markers, p-IRE1α, p-EIF2α and GRP78, were higher in the ovaries, COCs and GCs of PCOS mice than in those of control mice (Fig. 2F). The band intensities of the western blots are shown in Fig. 2G.

Metformin attenuates ER stress and concomitantly reduces p-p38 MAPK levels in DHT-treated PCOS mice

Metformin significantly reduced the body weights of DHT-treated mice and mildly improved the abnormal oestrous cycles, steroid hormone

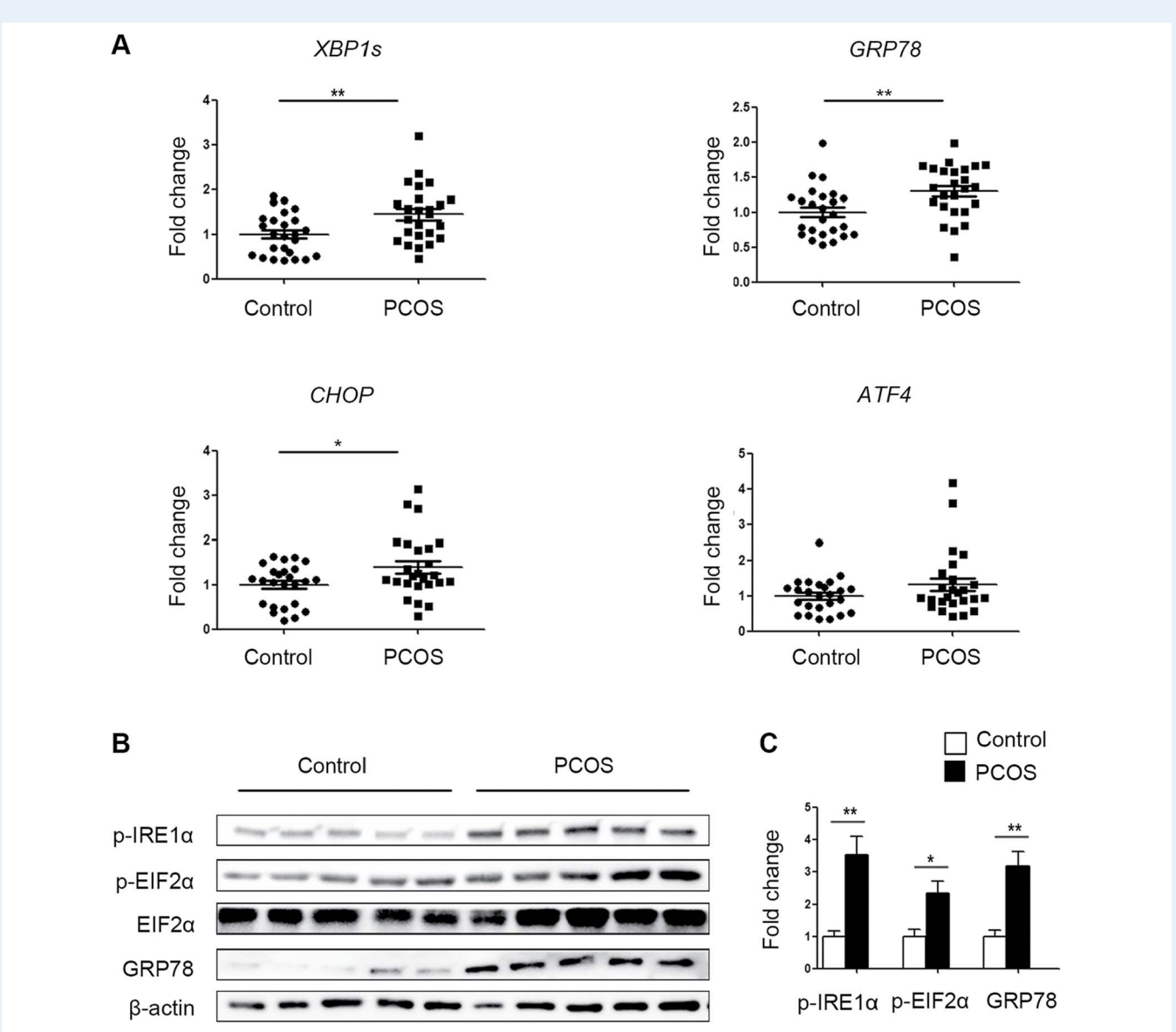

Figure 1 Comparison of endoplasmic reticulum (ER) stress activation in cumulus cells between polycystic ovary syndrome (PCOS) patients and control patients. (**A**) The expression of the unfolded protein response (UPR)-related genes *GRP78*, *XBP1s*, *CHOP*, and *ATF4* was analysed by real-time qPCR in PCOS patients and control patients ($n = 25$ per group). The mRNA expression levels were normalized to those of *Gapdh*. The data are presented as means ± SEMs. $^{*}P < 0.05$, $^{**}P < 0.01$. (**B**) The protein levels of p-IRE1α, p-EIF2α and GRP78 were assessed by western blot analysis of cumulus cells from randomly selected PCOS patients ($n = 5$) and control patients ($n = 5$). (**C**) The band intensities were determined with ImageJ software and normalized to those of β-actin, except those of p-EIF2α, which were normalized to those of total EIF2α. The data are presented as means ± SEMs. $^{*}P < 0.05$, $^{**}P < 0.01$.

levels and CL formation in these mice (Supplementary Table SII and Supplementary Fig. S1B–E). Additionally, metformin efficiently reduced serum TGC levels without changing CHOL levels (Supplementary Fig. S2G and H).

GCs from metformin-treated PCOS mouse ovaries showed reduced levels of *GRP78*, *CHOP*, *XBP1s* and *ATF4* expression, but COCs showed significant differences only for *GRP78 and XBP1s* (Fig. 3A and B). Consistent with the mRNA analysis results, the DHT-mediated elevations in p-IRE1α, p-EIF2α and GRP78 protein levels were attenuated by metformin in GCs (Fig. 3C and D) and COCs (Fig. 3E and F). Notably, the activity of p-p38 MAPK was increased in the GCs and COCs of DHT-treated mouse ovaries, but metformin efficiently reduced p-p38 MAPK activation (Fig. 3C–F).

Metformin reverses testosterone-induced ER stress by inactivating the p38 MAPK pathway in primary cultured GCs and COCs

The effects of various testosterone concentrations and treatment durations on primary cultured GCs were determined *in vitro* (Supplementary Fig. S3A–C). Administration of 10 μM testosterone

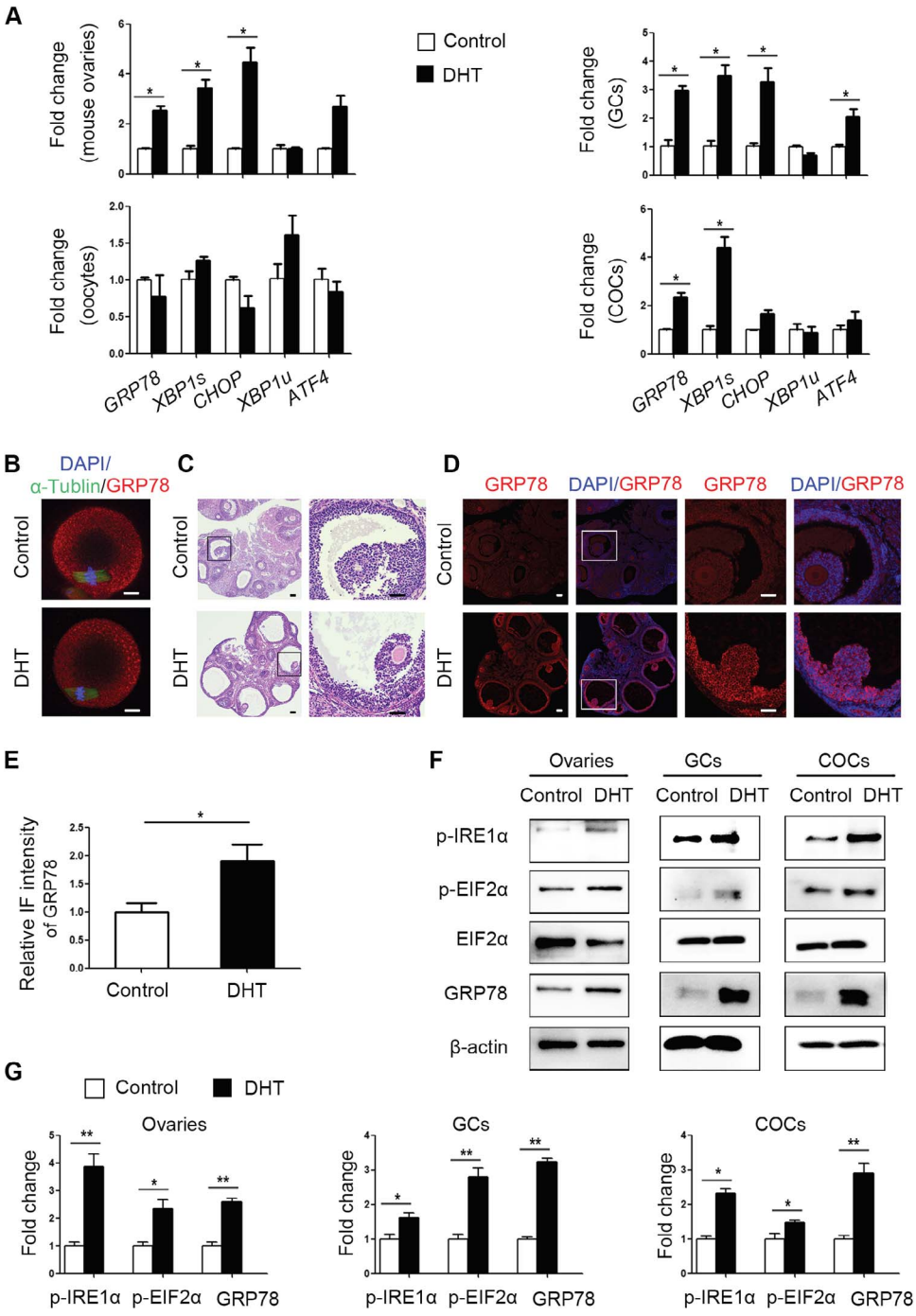

Figure 2 Expression patterns of unfolded protein response (UPR) genes and proteins in ovaries, cumulus oocyte complexes (COCs), oocytes and granulosa cells (GCs) of control and dihydrotestosterone (DHT)-treated polycystic ovary syndrome (PCOS) mice (*n* = 8 per treatment group). (**A**) *GRP78*, *XBP1s*, *XBP1u*, *CHOP* and *ATF4* mRNA expression levels in whole ovarian tissues, COCs, GCs and denuded oocytes were analysed by real-time qPCR, and the relative fold changes were calculated by normalization to the levels of *Gapdh*. The data are presented as means ± SEMs. $^{*}P < 0.05$. (**B**) Representative immunofluorescence (IF) images for GRP78 protein (red) in metaphase II oocytes from DHT-treated and control mice, with co-staining for FITC-α-tubulin (green, spindle) and DAPI (blue, chromosomes). Scale bar: 20 μm. (**C**) Histology of control and DHT-treated mouse ovaries. Scale bar: 100 μm. (**D**) Representative IF results showing GRP78 expression levels in control and DHT-treated mouse ovaries. Scale bar: 100 μm. (**E**) The relative intensities of IF levels calculated using ImageJ software in the two groups. The data are presented as means ± SEMs. $^{*}P < 0.05$. (**F**) Western blot results for p-IRE1α, p-EIF2α, total EIF2α and GRP78 protein levels in the ovaries, COCs and GCs of control and PCOS mice. (**G**) The band intensities were determined with ImageJ software and normalized to those of β-actin, except for those of p-EIF2α, which were normalized to those of total EIF2α. The data are presented as means ± SEMs. $^{*}P < 0.05$, $^{**}P < 0.01$. DHT, dihydrotestosterone; COCs, cumulus-oocyte complexes; GCs, granulosa cells; IF, immunofluorescence.

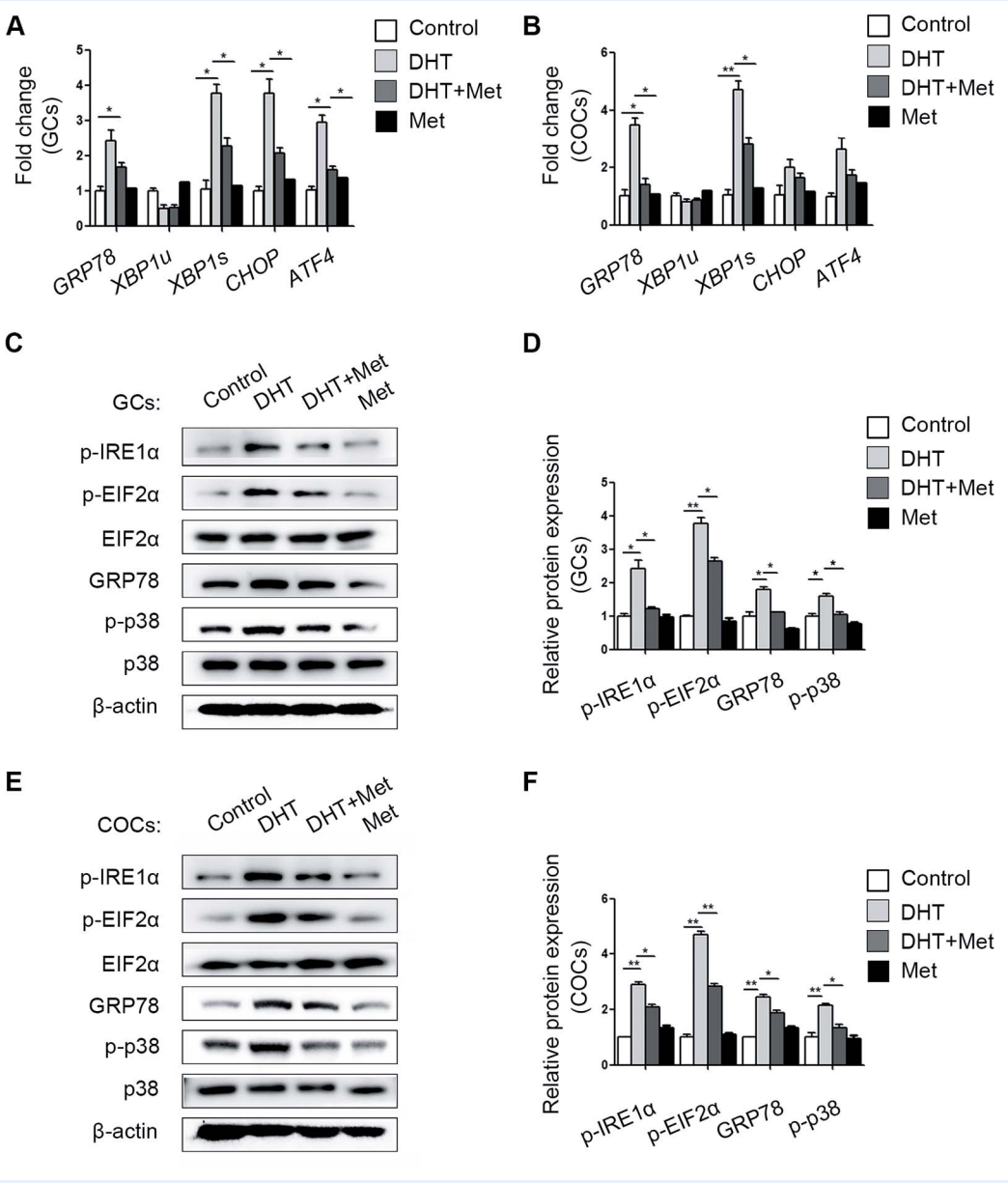

Figure 3 Different expression levels of unfolded protein response (UPR) genes and proteins in cumulus oocyte complexes (COCs) and granulosa cells (GCs) from different treatment groups ($n = 20$ per treatment group). *GRP78*, *XBP1s*, *XBP1u*, *CHOP* and *ATF4* mRNA expression levels in the GCs (**A**) and COCs (**B**) in the four groups were quantified by real-time qPCR and normalized to that of *Gapdh*. The data are presented as means ± SEMs. $^{*}P < 0.05$, $^{**}P < 0.01$. (**C**) The p-IRE1α, p-EIF2α, total EIF2α, GRP78, p-p38 MAPK and total p38 MAPK protein levels in GCs in the different groups were measured by western blot. (**D**) The band intensities in GCs were analysed with ImageJ software and normalized to those of β-actin, except those of p-p38 MAPK and p-EIF2α, which were normalized to those of total p38 MAPK and EIF2α, respectively. The data are presented as means ± SEMs. $^{*}P < 0.05$, $^{**}P < 0.01$. (**E**) Expression levels of the above proteins were measured in COCs by western blot. (**F**) The relative band intensities in COCs were analysed with ImageJ software. The data are presented as means ± SEMs. $^{*}P < 0.05$, $^{**}P < 0.01$. DHT, dihydrotestosterone; Met, metformin.

for 24 h was sufficient to trigger the expression of ER-stress-related mRNAs and proteins.

Consistent with our previous results, metformin mitigated the increase of p-IRE1α, p-EIF2α, GRP78 and p-p38 MAPK levels induced by testosterone in primary cultured GCs (Fig. 4A). SB203580, an inhibitor of p38 MAPK, was used to confirm that p38 MAPK plays a key role in testosterone-mediated activation of ER stress. SB203580 inhibits the catalytic activity of p38 MAPK by binding to the ATP-binding pocket but does not inhibit p38 MAPK phosphorylation (Supplementary Fig. S3D). As expected, the testosterone-mediated activation of ER stress, as were the levels of the p-IRE1α, p-EIF2α and GRP78 proteins in GCs (Fig. 4B) was reduced by SB203580. Furthermore, transfection of GCs with si-p38 MAPK also alleviated the testosterone-induced increases in ER stress-related proteins (Fig. 4C).

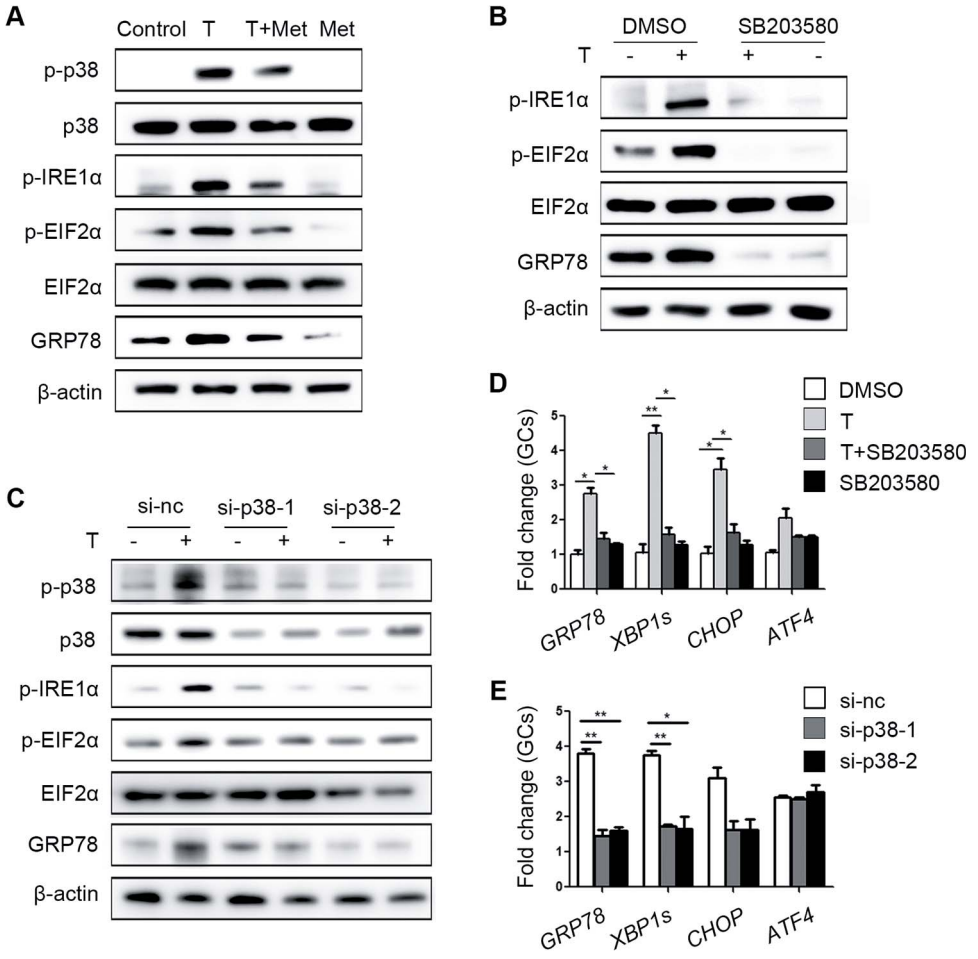

Figure 4 Ameliorative effects of metformin on testosterone-induced endoplasmic reticulum (ER) stress in mouse granulosa cells (GCs) mediated via reduction of p38 MAPK phosphorylation. (**A**) Unfolded protein response (UPR) sensor protein levels in GCs after treatment with 10 μM testosterone (T) and 1 mM metformin (met). (**B**) Protein changes in GCs treated with 10 μM testosterone and 10 μM SB203580 (a p38 MAPK inhibitor) as detected by western blot. (**C**) Western blot results showing the changes in the indicated proteins in GCs treated with 10 μM testosterone after transfection with si-p38 MAPK. (**D**, **E**) Effects of SB203580 (D) and si-p38 MAPK (E) on ER stress-related mRNA expression levels in GCs treated with 10 μM testosterone; the signals were normalized to those of *Gapdh*. The data are presented as means ± SEMs. $^{*}P < 0.05$, $^{**}P < 0.01$. Si-nc, negative control siRNA; Met, metformin; T, testosterone.

The testosterone-mediated elevations in ER stress-related mRNAs levels in GCs were also decreased by SB203580 and si-p38 MAPK treatment (Fig. 4D and E).

Similarly, activation of UPR-related proteins and p-p38 MAPK was observed in testosterone-treated COCs and was reduced by metformin (Fig. 5A). SB203580 and si-p38 MAPK efficiently reduced ER stress activation in COCs at the protein (Fig. 5B and C) and mRNA levels (Fig. 5D and E).

Testosterone alters the reaction of GCs and COCs to LH, but this alteration is mitigated by metformin, si-p38 MAPK or ER stress inhibitor

To analyse the direct effects of ER stress on the actions of LH in GCs, we measured transcriptional differences in LH-related genes, in the presence or absence of FSK/PMA. The epidermal growth factor (EGF)-like factors, amphiregulin (*Areg*) and epiregulin (*Ereg*) mediate the actions of LH in follicle development and maturation. Real-time qPCR showed that mRNA levels of *Areg* and *Ereg* were significantly upregulated in GCs treated with FSK/PMA (Fig. 6A). The expression of *Areg* and *Ereg* was further elevated by testosterone in the presence of FSK/PMA. Testosterone also increased the expression of genes required for cumulus cell expansion. These genes included: prostaglandin endoperoxide synthase 2 (*Ptgs2*), tumour necrosis factor alpha-induced protein 6 (*Tnfaip6*), pentraxin 3 (*Ptx3*) and oestrogen sulfotransferase (*Sult1e1*) (Fig. 6A). In the *in vitro* maturation experiments, testosterone-treated COC showed higher expression levels of the expansion-related genes than non-treated COCs (Fig. 6B).

However, metformin mitigated the expression of the ovulation-related genes *Ptgs2*, *Tnfaip6*, *Ptx3* and *Sult1e1* in GCs and COCs. To

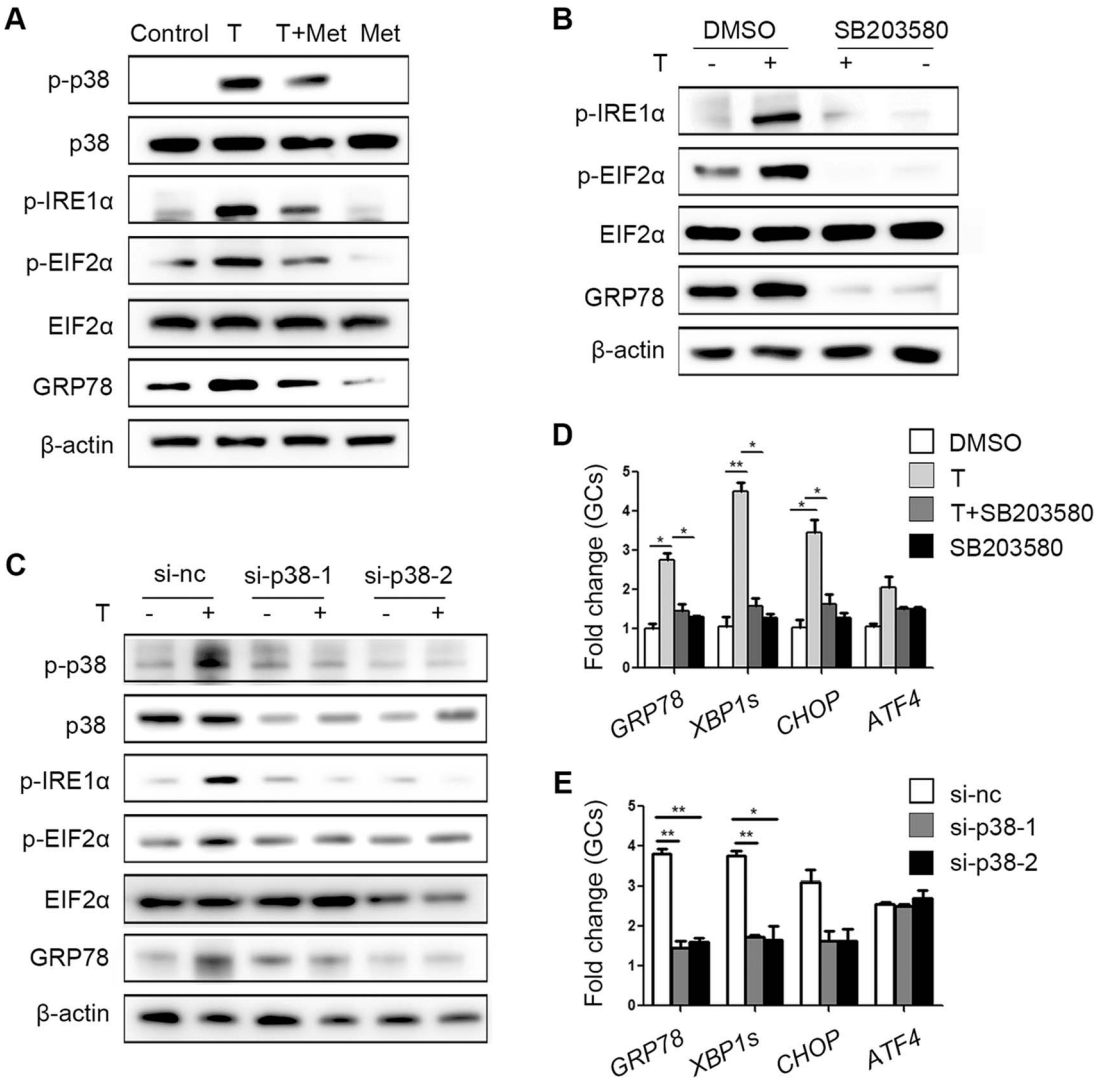

Figure 5 Ameliorative effects of metformin on testosterone-induced endoplasmic reticulum (ER) stress in cumulus oocyte complexes (COCs) mediated via reduction of p38 MAPK phosphorylation. (**A**) Unfolded protein response (UPR) sensor protein levels in COCs treated with 10 μM testosterone (T) and 1 mM metformin (met). (**B**) Changes in ER stress-related protein levels in COCs treated with 10 μM testosterone and 10 μM SB203580 (a p38 MAPK inhibitor) as detected by western blot. (**C**) Western blot results showing the changes in the indicated proteins in COCs treated with 10 μM testosterone after transfection with si-p38 MAPK. Real-time qPCR results showing the effects of SB203580 (**D**) and si-p38 MAPK (**E**) on ER stress-related mRNA transcription levels in COCs treated with 10 μM testosterone; the signals were normalized to those of *Gapdh*. The data are presented as means ± SEMs. $^{*}P < 0.05$, $^{**}P < 0.01$. Si-nc, negative control siRNA; Met, metformin; T, testosterone.

assess the role of p38 MAPK in testosterone-mediated LH target gene induction, we used si-p38 MAPK to inhibit p38 MAPK activity. The expression levels of *Areg*, *Ptgs2*, *Sult1e1*, *Ptx3* and *Tnfaip6* reduced when p38 MAPK expression was downregulated in GCs and COCs. TUDCA, an inhibitor of ER stress, alleviated the testosterone-induced overexpression of LH-related genes. In contrast, TG, an inducer of ER stress, upregulated the expression of *Areg*, *Ereg*, *Ptgs2*, *Tnfaip6*, *Ptx3* and *Sult1e1* (Fig. 6A and B).

Based on the results shown in Fig. 6C and D, COC expansion was accelerated in the presence of testosterone and TG, but this acceleration was slowed by treatment with metformin, si-p38 MAPK or TUDCA.

GC apoptosis in the antral follicles of DHT-treated mice is not induced by hyperandrogenism

To further clarify the roles of ER stress and apoptosis in hyperandrogenism, we measured cell apoptosis using several methods. Primary cultured GCs were treated with 10 μM testosterone with or without 1 mM metformin for 24 h and then analysed by PI and FITC-Annexin V staining followed by flow cytometry. The apoptosis rate of testosterone-treated GCs was 5% higher than that of control GCs. Metformin slightly attenuated this increase (Supplementary Fig. S4A and B). The cleaved PARP protein was also mildly increased in

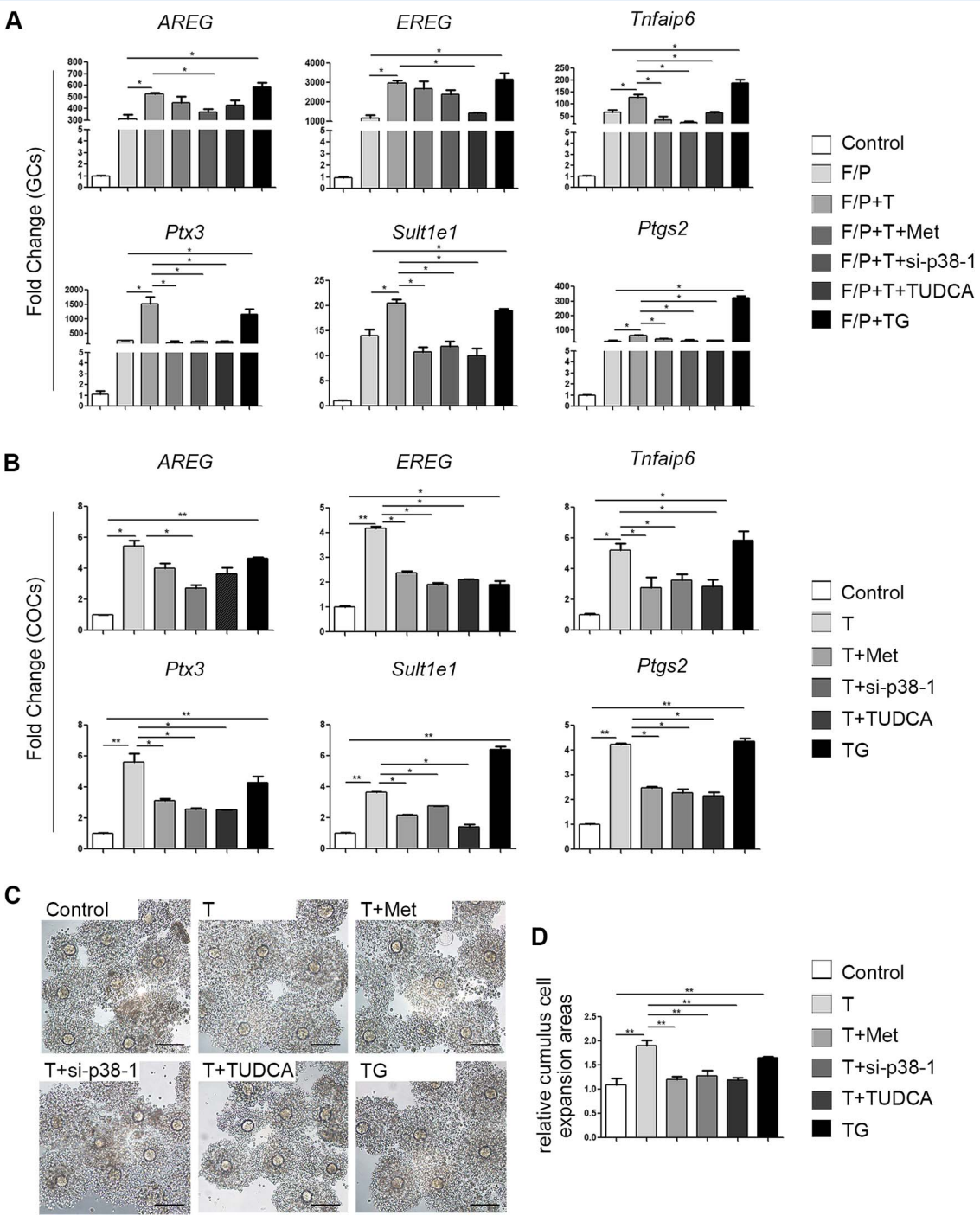

Figure 6 Effects of testosterone together with other drugs on LH responses in cultured granulosa cells (GCs) and cumulus oocyte complexes (COCs). (**A**) Real-time qPCR results showing the mRNA levels of the indicated genes (*Areg*, *Ereg*, *Tnfaip6*, *Ptx3*, *Sult1e1* and *Ptgs2*) in cultured GCs treated with 10 μM testosterone (T), 1 mM metformin (met), si-p38 MAPK, or 1 mg/ml tauroursodeoxycholic acid (TUDCA; an ER stress inhibitor) for 24 h or with 1 μM thapsigargin (TG; an ER stress inducer) for 1 h before treatment with forskolin (F; 10 μM) plus phorbol 12-myristate 13-acetate (P; 20 nM) for 4 h. The data are presented as means ± SEMs. $^{*}P < 0.05$. (**B**) Real-time qPCR results showing mRNA levels in cultured COCs after different treatments. The levels of specific mRNAs were normalized to the *Gapdh* signals. The data are presented as means ± SEMs. $^{*}P < 0.05$, $^{**}P < 0.01$. (**C**) COCs expansion after *in vitro* maturation in medium containing 10 μM testosterone and the drugs described above. (**D**) Histograms of the COC expansion areas made with ImageJ software. The data are presented as means ± SEMs. $^{**}P < 0.01$. Scale bar = 100 μm. GCs, granulosa cells; COCs, cumulus-oocyte complexes; F/P, forskolin and phorbol 12-myristate 13-acetate; T, testosterone; Met, metformin; TUDCA, tauroursodeoxycholic acid; TG, thapsigargin.

the testosterone-treated GCs (Supplementary Fig. S4C). We further performed TUNEL analysis and measured the levels of cleaved caspase 3 on ovarian sections of control mice, DHT-treated mice and DHT- and metformin-treated mice. Apoptotic signals were low in all samples, and there were no obvious differences between the control and DHT-treated groups (Supplementary Fig. S4D and E). These results indicate that GC apoptosis in the antral follicles of DHT-treated mice is not markedly induced by hyperandrogenism.

Discussion

PCOS is a syndrome associated with metabolic and endocrine abnormalities. Hyperandrogenism is a key feature of PCOS (Rosenfield and Ehrmann, 2016; Lim *et al*., 2019). Although in our study, the serum testosterone levels of the PCOS patients and control patients were not significantly different, the ovaries of the PCOS patients exhibited hyperandrogenic follicular environments (Table I). Another study also reported higher follicular fluid testosterone levels in PCOS patients than in healthy subjects. This difference was not changed by pituitary suppression and exogenous FSH treatment in ovulation-stimulated patients (Yang *et al*., 2015). Given these findings, investigating the consequences of hyperandrogenism within follicles is essential.

Recent studies have shown that testosterone-induced ER stress leads to apoptosis of human and mouse cumulus cells (Azhary *et al*., 2019). In our study, we performed a series of experiments to measure hyperandrogenism-mediated apoptosis, and the results are shown in Supplementary Fig. S4. However, the apoptosis rates and apoptosis signals in the antral follicles of the hyperandrogenic groups were slightly but non-significantly increased. We speculate that the testosterone concentration used to treat the GCs was not high enough to exert a significant effect, even though the concentration was several-fold higher than that in the follicular fluid of PCOS patients. Additionally, we used DHT slow-release implants rather than daily injections of dehydroepiandrosterone to establish the PCOS mouse model, which might account for the existence of high levels of ER stress without high levels of apoptosis. Thus, we infer that low testosterone concentrations result in ER stress and that high testosterone concentrations lead to GC apoptosis in PCOS patients.

In our study, hyperandrogenism-induced ER stress in the GCs and COCs of a PCOS mouse model but not in oocytes. A previous study has shown that UPR signalling and ER stress also play important roles in ovarian follicle development (Harada *et al*., 2015). Another study showed that melatonin-mediated suppression of ER stress in COCs improves the meiotic maturation of porcine oocytes (Park *et al*., 2018). Moreover, ER stress in mouse COCs impairs protein secretion, mitochondrial activity, and oocyte developmental competence (Wu *et al*., 2012). We speculate that hyperandrogenism leads to cumulus cell dysfunction that indirectly impairs oocyte competence in PCOS patients.

Over the last 20 years, metformin has been widely used to treat PCOS patients, especially those with metabolic and reproductive abnormalities. Recent studies have shown that metformin treatment may increase ovulation and reduce serum testosterone levels primarily by preventing excessive insulin actions in the ovaries (Palomba *et al*., 2009; Hirsch *et al*., 2012; Kurzthaler *et al*., 2014; Morley *et al*., 2017; Sam and Ehrmann, 2017). Metformin has also been found to increase insulin sensitization, alleviate metabolic disorders and improve polycystic symptoms in mice by activating the adenosine monophosphate-activated protein kinase (AMPK) signalling pathway (Carvajal *et al*., 2013; Tan *et al*., 2013; Chen *et al*., 2019). Except AMPK pathway, recent studies demonstrated that metformin reduces inflammation associated with bowel diseases, preterm birth and renal fibrosis in humans and mice by inhibiting the p38 MAPK signalling pathways (Di Fusco *et al*., 2018; Sun *et al*., 2018; Yi *et al*., 2018). A recent report has shown that the p38 MAPK signalling pathway is associated with ER stress activation (Govindarajan *et al*., 2018; Li *et al*., 2018; Kim *et al*., 2019). In addition, under severe or sustained ER stress, p38 MAPK phosphorylation leads to cell dysfunction (Tobiume *et al*., 2001). Therefore, we reasonably hypothesize that hyperandrogenism activates ER stress via the p38 MAPK pathway and that this effect is disrupted by metformin.

Previous studies have shown the abnormal steroidogenesis and altered gene expression in the cumulus cells of PCOS patients (Haouzi *et al*., 2012; Schmidt *et al*., 2014). Although gene expression profiles in cumulus cells between PCOS patients and individuals without PCOS have been compared in previous studies (Haouzi *et al*., 2012; Schmidt *et al*., 2014), the expression of *Areg*, *Ereg*, *Ptgs2*, *Sult1e1*, *Tnfaip6* and *Ptx3* was not evaluated. Besides, we observed that TG, an ER stress inducer, activated COC expansion-related gene expression excessively. However, TUDCA, an ER stress inhibitor, was able to mitigate the abnormal expression of these genes induced by testosterone. Based on these results, we speculated that the alteration of gene expression in PCOS patients may be partially caused by hyperandrogenism-induced ER stress. However, whether ER stress contributes to the pathogenesis of PCOS needs further investigation.

Taken together, our study demonstrates that metformin is able to alleviate testosterone-induced ER stress by inhibiting p38 MAPK phosphorylation. These observations indicate that metformin treatment may be beneficial for PCOS patients.

Supplementary data

Supplementary data are available at *Human Reproduction* online.

Acknowledgements

We thank all the patients who participated in our research. We are also grateful to Professor Jeffrey M. Goldberg from Cleveland Clinic for language editing supports. We sincerely thank the assisted reproductive technology team at Sir Run Run Shaw Hospital.

Authors' roles

J.J. and Y.M. performed the acquisition, analysis and interpretation of the data and drafted the article. S.Z. and Y.Z. conceived the study and revised the manuscript critically. X.T. and W.Y. collected human samples. All the other authors, who conducted additional data acquisition and analysis, were heavily involved in the intellectual study design, acquisition and interpretation of data, critical revision of the article and approval of the paper for final submission.

Funding

National Key Research and Developmental Program of China (2018YFC1004800); Key Research and Development Program of Zhejiang Province (2017C03022); Zhejiang Province Medical Science and Technology Plan Project (2017KY085, 2018KY457); National Natural Science Foundation of China (31701260, 81401264, 81701514); Special Funds for Clinical Medical Research of Chinese Medical Association (16020320648).

Conflict of interest

The authors declare that they have no conflicts of interest in the authorship or publication of this study.

References

Azhary JMK, Harada M, Takahashi N, Nose E, Kunitomi C, Koike H, Hirata T, Hirota Y, Koga K, Wada-Hiraike O *et al*. Endoplasmic reticulum stress activated by androgen enhances apoptosis of granulosa cells via induction of death receptor 5 in PCOS. *Endocrinology* 2019;**160**:119–132.

Barrea L, Marzullo P, Muscogiuri G, Di Somma C, Scacchi M, Orio F, Aimaretti G, Colao A, Savastano S. Source and amount of carbohydrate in the diet and inflammation in women with polycystic ovary syndrome. *Nutr Res Rev* 2018;**31**:291–301.

Bozdag G, Mumusoglu S, Zengin D, Karabulut E, Yildiz BO. The prevalence and phenotypic features of polycystic ovary syndrome: a systematic review and meta-analysis. *Hum Reprod* 2016;**31**:2841–2855.

Caldwell ASL, Edwards MC, Desai R, Jimenez M, Gilchrist RB, Handelsman DJ, Walters KA. Neuroendocrine androgen action is a key extraovarian mediator in the development of polycystic ovary syndrome. *Proc Natl Acad Sci U S A* 2017;**114**:E3334–E3343.

Carvajal R, Rosas C, Kohan K, Gabler F, Vantman D, Romero C, Vega M. Metformin augments the levels of molecules that regulate the expression of the insulin-dependent glucose transporter GLUT4 in the endometria of hyperinsulinemic PCOS patients. *Hum Reprod* 2013;**28**:2235–2244.

Chen Z, Wei H, Zhao X, Xin X, Peng L, Ning Y, Wang Y, Lan Y, Zhang Q. Metformin treatment alleviates polycystic ovary syndrome by decreasing the expression of MMP-2 and MMP-9 via H19/miR-29b-3p and AKT/mTOR/autophagy signaling pathways. *J Cell Physiol* 2019;**234**:19964–19976.

Cree LM, Hammond ER, Shelling AN, Berg MC, Peek JC, Green MP. Maternal age and ovarian stimulation independently affect oocyte mtDNA copy number and cumulus cell gene expression in bovine clones. *Hum Reprod* 2015;**30**:1410–1420.

Di Fusco D, Dinallo V, Monteleone I, Laudisi F, Marafini I, Franze E, Di Grazia A, Dwairi R, Colantoni A, Ortenzi A *et al*. Metformin inhibits inflammatory signals in the gut by controlling AMPK and p38 MAP kinase activation. *Clin Sci* 2018;**132**:1155–1168.

El-Mir MY, Nogueira V, Fontaine E, Averet N, Rigoulet M, Leverve X. Dimethylbiguanide inhibits cell respiration via an indirect effect targeted on the respiratory chain complex I. *J Biol Chem* 2000;**275**:223–228.

Govindarajan S, Gaublomme D, Van der Cruyssen R, Verheugen E, Van Gassen S, Saeys Y, Tavernier S, Iwawaki T, Bloch Y, Savvides SN *et al*. Stabilization of cytokine mRNAs in iNKT cells requires the serine-threonine kinase IRE1alpha. *Nat Commun* 2018;**9**:5340.

Haouzi D, Assou S, Monzo C, Vincens C, Dechaud H, Hamamah S. Altered gene expression profile in cumulus cells of mature MII oocytes from patients with polycystic ovary syndrome. *Hum Reprod* 2012;**27**:3523–3530.

Harada M, Nose E, Takahashi N, Hirota Y, Hirata T, Yoshino O, Koga K, Fujii T, Osuga Y. Evidence of the activation of unfolded protein response in granulosa and cumulus cells during follicular growth and maturation. *Gynecol Endocrinol* 2015;**31**:783–787.

Hirsch A, Hahn D, Kempna P, Hofer G, Nuoffer JM, Mullis PE, Fluck CE. Metformin inhibits human androgen production by regulating steroidogenic enzymes HSD3B2 and CYP17A1 and complex I activity of the respiratory chain. *Endocrinology* 2012;**153**:4354–4366.

Insenser M, Montes-Nieto R, Murri M, Escobar-Morreale HF. Proteomic and metabolomic approaches to the study of polycystic ovary syndrome. *Mol Endocrinol* 2013;**370**:65–77.

Jia L, Zeng Y, Hu Y, Liu J, Yin C, Niu Y, Wang C, Li J, Jia Y, Hong J *et al*. Homocysteine impairs porcine oocyte quality via deregulation of one carbon metabolism and hypermethylation of mitochondrial DNA. *Biol Reprod* 2019;**100**:907–916.

Kim HS, Kim Y, Lim MJ, Park YG, Park SI, Sohn J. The p38-activated ER stress-ATF6alpha axis mediates cellular senescence. *FASEB J* 2019;**33**:2422–2434.

Kozutsumi Y, Segal M, Normington K, Gething MJ, Sambrook J. The presence of malfolded proteins in the endoplasmic reticulum signals the induction of glucose-regulated proteins. *Nature* 1988;**332**:462–464.

Kurzthaler D, Hadziomerovic-Pekic D, Wildt L, Seeber BE. Metformin induces a prompt decrease in LH-stimulated testosterone response in women with PCOS independent of its insulin-sensitizing effects. *Reprod Biol Endocrinol* 2014;**12**:98.

Lee HM, Kim CW, Hwang KA, Sung JH, Lee JK, Choi KC. Cigarette smoke impaired maturation of ovarian follicles and normal growth of uterus inner wall of female wild-type and hypertensive rats. *Reprod Toxicol* 2017;**73**:232–240.

Lee MS, Kang SK, Lee BC, Hwang WS. The beneficial effects of insulin and metformin on in vitro developmental potential of porcine oocytes and embryos. *Biol Reprod* 2005;**73**:1264–1268.

Li W, Yang Q, Mao Z. Signaling and induction of chaperone-mediated autophagy by the endoplasmic reticulum under stress conditions. *Autophagy* 2018;**14**:1094–1096.

Lim SS, Kakoly NS, Tan JWJ, Fitzgerald G, Bahri Khomami M, Joham AE, Cooray SD, Misso ML, Norman RJ, Harrison CL *et al*. Metabolic syndrome in polycystic ovary syndrome: a systematic review, meta-analysis and meta-regression. *Obes Rev* 2019;**20**:339–352.

Liu J, Luo LF, Wang DL, Wang WX, Zhu JL, Li YC, Chen NZ, Huang HL, Zhang WC. Cadmium induces ovarian granulosa cell damage by activating PERK-eIF2alpha-ATF4 through endoplasmic reticulum stress. *Biol Reprod* 2019;**100**:292–299.

Lizneva D, Suturina L, Walker W, Brakta S, Gavrilova-Jordan L, Azziz R. Criteria, prevalence, and phenotypes of polycystic ovary syndrome. *Fertil Steril* 2016;**106**:6–15.

Luque-Ramirez M, Nattero-Chavez L, Ortiz Flores AE, Escobar-Morreale HF. Combined oral contraceptives and/or antiandrogens

versus insulin sensitizers for polycystic ovary syndrome: a systematic review and meta-analysis. *Hum Reprod Update* 2018;**24**:225–241.

Maurel M, Chevet E, Tavernier J, Gerlo S. Getting RIDD of RNA: IRE1 in cell fate regulation. *Trends Biochem Sci* 2014;**39**:245–254.

Miller RA, Chu Q, Xie J, Foretz M, Viollet B, Birnbaum MJ. Biguanides suppress hepatic glucagon signalling by decreasing production of cyclic AMP. *Nature* 2013;**494**:256–260.

Morley LC, Tang T, Yasmin E, Norman RJ, Balen AH. Insulin-sensitising drugs (metformin, rosiglitazone, pioglitazone, D-chiro-inositol) for women with polycystic ovary syndrome, oligo amenorrhoea and subfertility. *The Cochrane database Syst Rev* 2017;**11**:CD003053.

Naderpoor N, Shorakae S, de Courten B, Misso ML, Moran LJ, Teede HJ. Metformin and lifestyle modification in polycystic ovary syndrome: systematic review and meta-analysis. *Hum Reprod Update* 2016;**22**:408–409.

Nestler JE, Jakubowicz DJ. Decreases in ovarian cytochrome P450c17 alpha activity and serum free testosterone after reduction of insulin secretion in polycystic ovary syndrome. *N Engl J Med* 1996;**335**:617–623.

Oakes SA, Papa FR. The role of endoplasmic reticulum stress in human pathology. *Annu Rev Pathol* 2015;**10**:173–194.

Palomba S, Falbo A, Zullo F, Orio F Jr. Evidence-based and potential benefits of metformin in the polycystic ovary syndrome: a comprehensive review. *Endo Rev* 2009;**30**:1–50.

Park HJ, Park JY, Kim JW, Yang SG, Jung JM, Kim MJ, Kang MJ, Cho YH, Wee G, Yang HY *et al*. Melatonin improves the meiotic maturation of porcine oocytes by reducing endoplasmic reticulum stress during in vitro maturation. *J Pineal Res* 2018;**64**:e12458.

Qiao J, Feng HL. Extra- and intra-ovarian factors in polycystic ovary syndrome: impact on oocyte maturation and embryo developmental competence. *Hum Reprod Update* 2011;**17**:17–33.

Rosenfield RL, Ehrmann DA. The pathogenesis of polycystic ovary syndrome (PCOS): the hypothesis of PCOS as functional ovarian hyperandrogenism revisited. *Endocr Rev* 2016;**37**:467–520.

Rotterdam EA-SPCWG. Revised 2003 consensus on diagnostic criteria and long-term health risks related to polycystic ovary syndrome. *Fertil Steril* 2004;**81**:19–25.

Sam S, Ehrmann DA. Metformin therapy for the reproductive and metabolic consequences of polycystic ovary syndrome. *Diabetologia* 2017;**60**:1656–1661.

Samuel SM, Ghosh S, Majeed Y, Arunachalam G, Emara MM, Ding H, Triggle CR. Metformin represses glucose starvation induced autophagic response in microvascular endothelial cells and promotes cell death. *Biochem Pharmacol* 2017;**132**:118–132.

Schmidt J, Weijdegard B, Mikkelsen AL, Lindenberg S, Nilsson L, Brannstrom M. Differential expression of inflammation-related genes in the ovarian stroma and granulosa cells of PCOS women. *Mol Hum Reprod* 2014;**20**:49–58.

Shore GC, Papa FR, Oakes SA. Signaling cell death from the endoplasmic reticulum stress response. *Curr Opin Cell Biol* 2011;**23**:143–149.

Sun X, Tavenier A, Deng W, Leishman E, Bradshaw HB, Dey SK. Metformin attenuates susceptibility to inflammation-induced preterm birth in mice with higher endocannabinoid levels. *Biol Reprod* 2018;**98**:208–217.

Tan BK, Chen J, Adya R, Ramanjaneya M, Patel V, Randeva HS. Metformin increases the novel adipokine adipolin/CTRP12: role of the AMPK pathway. *J Endocrinol* 2013;**219**:101–108.

Tobiume K, Matsuzawa A, Takahashi T, Nishitoh H, Morita K, Takeda K, Minowa O, Miyazono K, Noda T, Ichijo H. ASK1 is required for sustained activations of JNK/p38 MAP kinases and apoptosis. *EMBO Rep* 2001;**2**:222–228.

Vasickova K, Moran L, Gurin D, Vanhara P. Alleviation of endoplasmic reticulum stress by tauroursodeoxycholic acid delays senescence of mouse ovarian surface epithelium. *Cell Tissue Res* 2018;**374**:643–652.

Walter P, Ron D. The unfolded protein response: from stress pathway to homeostatic regulation. *Science* 2011;**334**:1081–1086.

Wang M, Kaufman RJ. Protein misfolding in the endoplasmic reticulum as a conduit to human disease. *Nature* 2016;**529**:326–335.

Wu LL, Russell DL, Norman RJ, Robker RL. Endoplasmic reticulum (ER) stress in cumulus-oocyte complexes impairs pentraxin-3 secretion, mitochondrial membrane potential and embryo development. *Mol Endocrinol* 2012;**26**:562–573.

Wu Y, Li Y, Liao X, Wang Z, Li R, Zou S, Jiang T, Zheng B, Duan P, Xiao J. Diabetes induces abnormal ovarian function via triggering apoptosis of granulosa cells and suppressing ovarian angiogenesis. *Int J Biol Sci* 2017;**13**:1297–1308.

Yang F, Ruan YC, Yang YJ, Wang K, Liang SS, Han YB, Teng XM, Yang JZ. Follicular hyperandrogenism downregulates aromatase in luteinized granulosa cells in polycystic ovary syndrome women. *Reproduction* 2015;**150**:289–296.

Yi H, Huang C, Shi Y, Cao Q, Zhao Y, Zhang L, Chen J, Pollock CA, Chen XM. Metformin attenuates folic-acid induced renal fibrosis in mice. *J Cell Physiol* 2018;**233**:7045–7054.

Zhang YL, Xia Y, Yu C, Richards JS, Liu J, Fan HY. CBP-CITED4 is required for luteinizing hormone-triggered target gene expression during ovulation. *Mol Hum Reprod* 2014;**20**:850–860.

Zhang YL, Yu C, Ji SY, Li XM, Zhang YP, Zhang D, Zhou D, Fan HY. TOP2beta is essential for ovarian follicles that are hypersensitive to chemotherapeutic drugs. *Mol Endocrinol* 2013;**27**:1678–1691.